Photo-mediated ring contraction of saturated heterocycles

Justin Jurczyk,[†‡] Michaelyn C. Lux,[§‡] Donovon Adpressa,[€] Sojung F. Kim,[†] Yu-hong Lam,[*¥] Charles S. Yeung,[*‖] Richmond Sarpong[*†]

† Department of Chemistry, University of California, Berkeley, CA 94720, United States.

§ MRL Postdoctoral Fellow, Discovery Chemistry, Merck & Co., Inc., 33 Avenue Louis Pasteur, Boston, MA 02115, United States.

¥ Computational and Structural Chemistry, Merck & Co., Inc., 90 E. Scott Avenue, Rahway, NJ 07065, United States.

€ Analytical Research & Development, Merck & Co., Inc., 33 Avenue Louis Pasteur, Boston, MA 02115, United States.

‖ Disruptive Chemistry Fellow, Discovery Chemistry, Merck & Co., Inc., 33 Avenue Louis Pasteur, Boston, MA 02115, United States.

Keywords: Cyclic amines, ring contraction, molecular editing, scaffold hop, Norrish Type II

‡These authors contributed equally to this work.

*Corresponding Author, email: yu.hong.lam@merck.com

*Corresponding Author, email: charles.yeung@merck.com

*Corresponding Author, email: rsarpong@berkeley.edu

Abstract: Saturated heterocycles are found in numerous therapeutics as well as bioactive natural products and are abundant in many medicinal and agrochemical compound libraries. In order to access new chemical space and function, many methods for functionalization on the periphery of these structures have been developed. Comparatively fewer methods are known for restructuring their core framework. Herein, we describe a visible light-mediated ring contraction of α-acylated saturated heterocycles. This unconventional transformation is orthogonal to traditional ring contractions, challenging the paradigm for diversification of heterocycles including piperidine, morpholine, thiane, tetrahydropyran, and tetrahydroisoquinoline derivatives. The success of this Norrish Type II variant rests on reactivity differences between photoreactive ketone groups in unique chemical environments. This strategy was applied to late-stage remodeling of pharmaceutical derivatives, peptides, and sugars.

One-Sentence Summary: A photo-mediated method that effects ring contraction of α-acylated heterocyclic frameworks is reported.

Saturated heterocycles, especially piperidines, are among the most frequently encountered scaffolds in biologically active small molecules (*1,2*). The prevalence of the piperidine scaffold in pharmaceutical and agrochemical compound libraries has resulted in increased interest in the development of methods for its site-selective derivatization (Fig. 1A) in order to access new chemical space. Recent advancements in C(sp^3)–H functionalization have provided many powerful methods for peripheral functionalization of the piperidine framework (*3–12*), shifting the paradigm in late-stage-functionalization. In comparison, methods that modify the piperidine skeleton are less abundant, prompting a quest for methods for this purpose. Such methods would be especially valuable for drug discovery, where maximizing structural diversity, specifically at a late stage, is highly valued (*13*). To this end, we sought to develop a ring contraction of piperidines and related saturated heterocycles to carbocyclic frameworks to achieve core, rather than peripheral, modification.

Relatively few methods for piperidine ring contraction exist as compared to those available for the ring contraction of carbocycles bearing functional handles. For example, in cyclohexanone derivatives alone, anionic, carbene, and cationic intermediates have all been exploited to achieve ring contraction. In contrast, for saturated nitrogen-containing heterocycles (azacycles), commonly employed ring contraction strategies predominantly leverage bicyclic, quaternary-ammonium intermediates, which undergo a formal ring contraction upon attack from an exogenous nucleophile (Fig. 1B) (*14, 15*). More recently, we reported an approach to piperidine ring contraction via oxidative C(sp^3)–N bond cleavage, wherein silver-mediated deconstructive bromination of *N*-benzoyl piperidines followed by intramolecular C–N bond reformation in the resulting acyclic bromoamine furnishes the corresponding N-benzoyl pyrrolidine scaffolds in two steps (Fig. 1B) (*16*). Though useful, these tactics are limited to piperidine-to-pyrrolidine scaffold conversions, require specific substitution patterns (*14, 15*), and employ strongly oxidizing conditions that pose a challenge for late-stage diversification (*16, 17*). The ring contractions of unsaturated azacyclic systems such as pyridiniums and dihydropyridines have also been explored, for example using light (*18,19*). However, these transformations are limited to substrates with well-recognized photoreactivity profiles.

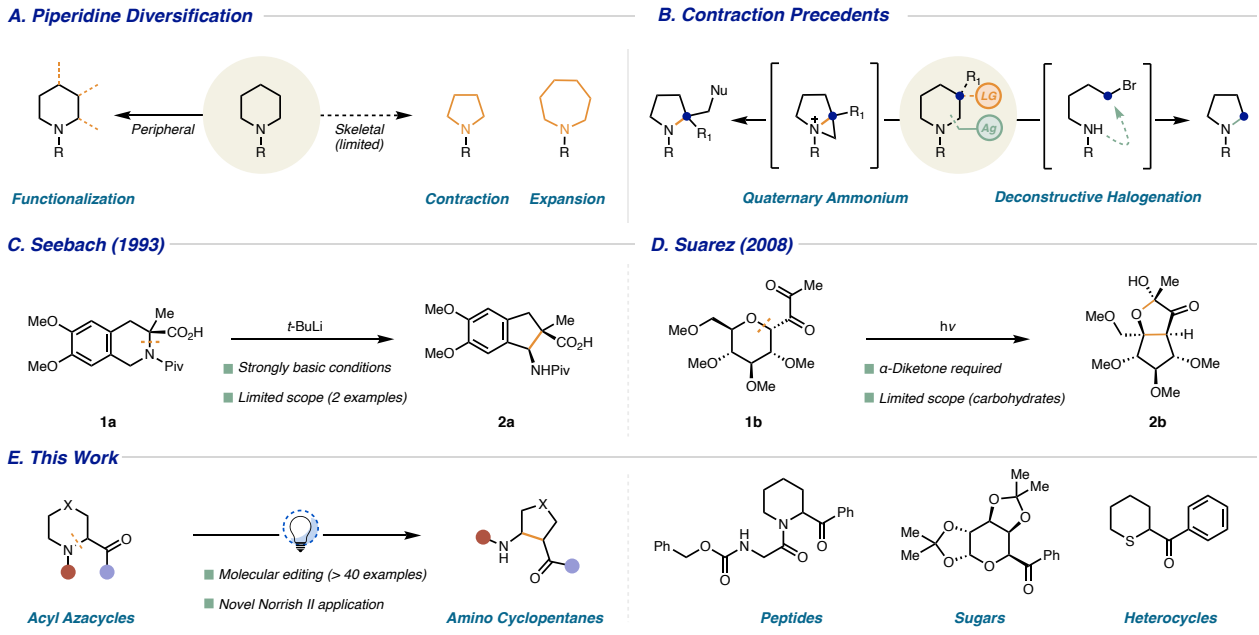

Figure 1. Approaches to piperidine diversification. (A) Peripheral functionalization and skeletal remodeling. (B) Selected examples of ring contractions on piperidine frameworks. (C) Seminal report of Seebach's unusual THIQ ring

contraction. (D) Contraction of carbohydrates reported by Suarez and coworkers. (E) Norrish Type II-approach to piperidine skeletal framework modification (*this work*).

We sought to develop a complementary and mechanistically distinct approach to piperidine ring contraction that could also be applied to a wide range of saturated heterocycles to provide access to underexplored, skeletally diverse substrates. We drew inspiration from an unusual transformation reported by Seebach and coworkers (Fig. 1C) wherein an α-carboxyl tetrahydroisoquinoline (THIQ) derivative (**1a**) underwent contraction to the corresponding indane scaffold (**2a**) under strongly basic conditions. This transformation features a curious endo-to-exocyclic nitrogen atom transposition, giving rise to a β-amino acid structural motif (*20*). Despite its novelty, only two examples were reported, and the requisite strongly basic conditions limit its potential application to skeletal modification of drug-like molecules bearing base-reactive functional groups. A more functional-group-compatible, albeit similarly specific, variant of this type of transformation was reported by Suarez for α-diketonyl sugars (e.g., **1b**), which undergo light-mediated ring contraction with a subsequent hemiketalization to give fused [5,5] ring systems (i.e., **2b**) (Fig. 1D) (*21, 22*). Notably, the α-diketone moiety required for the reaction is derivatized in the resulting product. Our design of a complementary ring contraction sought broad functional group compatibility and a widened scope beyond α-diketonyl-derived sugars. Herein, we report the visible-light mediated ring contraction of α-acylated cyclic piperidines to furnish *cis*-1,2-disubstituted cyclopentane scaffolds (Fig. 1E) and the extension of this method to other saturated heterocycles including tetrahydropyrans and thianes. The success of these Norrish Type II transformations hinged on predicted (and observed) photophysical differences between the ketone groups in the starting substrates and products (*vide infra*). An asymmetric variant of this transformation is also disclosed.

Development of Photo-Mediated Ring Contraction

We commenced our studies by focusing on piperidine ring contractions (Fig. 2A). We envisioned that upon irradiation, α-acylated precursors such as **I**, where the aroyl group is disposed pseudo axially to avoid pseudo $A^{1,3}$-like strain (*23*), would undergo excitation and intersystem crossing (ISC) to afford **II** in the triplet state. A subsequent Norrish Type II 1,5-hydrogen atom abstraction (HAT) would yield the corresponding 1,4-diradical (**III**), which would undergo homolytic C–N bond fragmentation, leading to imine-enol **IV**. The desired cyclopentane product would then result from an intramolecular enol attack on the tethered imine (Mannich reaction) to afford cyclopentane **V**. Under photo-irradiation, however, we also recognized the potential for undesired reactivity (Fig. 2B), especially further reactivity of the reaction product (**V**) to form additional excited species such as **VI**.

In principle, the success of the reaction would depend on subtle differences in reactivity between the starting material (**I**) and the reaction product (**V**; an anticipated "photo-stationary" state), as both bear a photoreactive phenyl ketone that could participate in Norrish-type processes (see **VI**). In their studies (Fig. 1D), (*21, 22*) Suarez and coworkers had achieved success primarily because a photo-stationary state was reached upon hemiketalization of the α-diketone in the product. We envisioned that even though chemical transformation of the photoreactive moiety would not be realized upon product formation in our case, differences in the $n\rightarrow\pi^*$ photo-absorption profiles of **I** and **V** could arise by virtue of an intramolecular hydrogen bond that is established in **V**. As is well known for spatially forbidden $n\rightarrow\pi^*$ transitions, increased

polarity in the local environment can lead to a hypsochromic (blue) shift for λ_{max} (*24*), which we anticipated would lead to differences in the photoreactivity of **I** and **V**. Additionally, we recognized that other photochemical processes could outcompete our desired ring contraction reaction. For example, though more prominent for dialkyl ketones, Norrish Type I carbon–carbon bond homolysis from the triplet excited state (i.e., **II**) could lead to formation of undesired alkyl-acyl radical pairs (see **VII**) (*24*). Another possible complication could arise following 1,5-hydrogen atom abstraction, where radical recombination of diradical **III** could occur to give the corresponding [3.1.1]-bicycle (**VIII**), i.e., a Norrish–Yang cyclization. We imagined that a Norrish Type II C–N fragmentation of **III** (to ultimately afford **V**) would outcompete a Norrish–Yang cyclization on the basis of an anticipated unfavorable conformational bias against ring closure to azetidinol **VIII** and a slower rate for intersystem crossing to the requisite singlet diradical for cyclobutanol C–C bond formation (*25*).

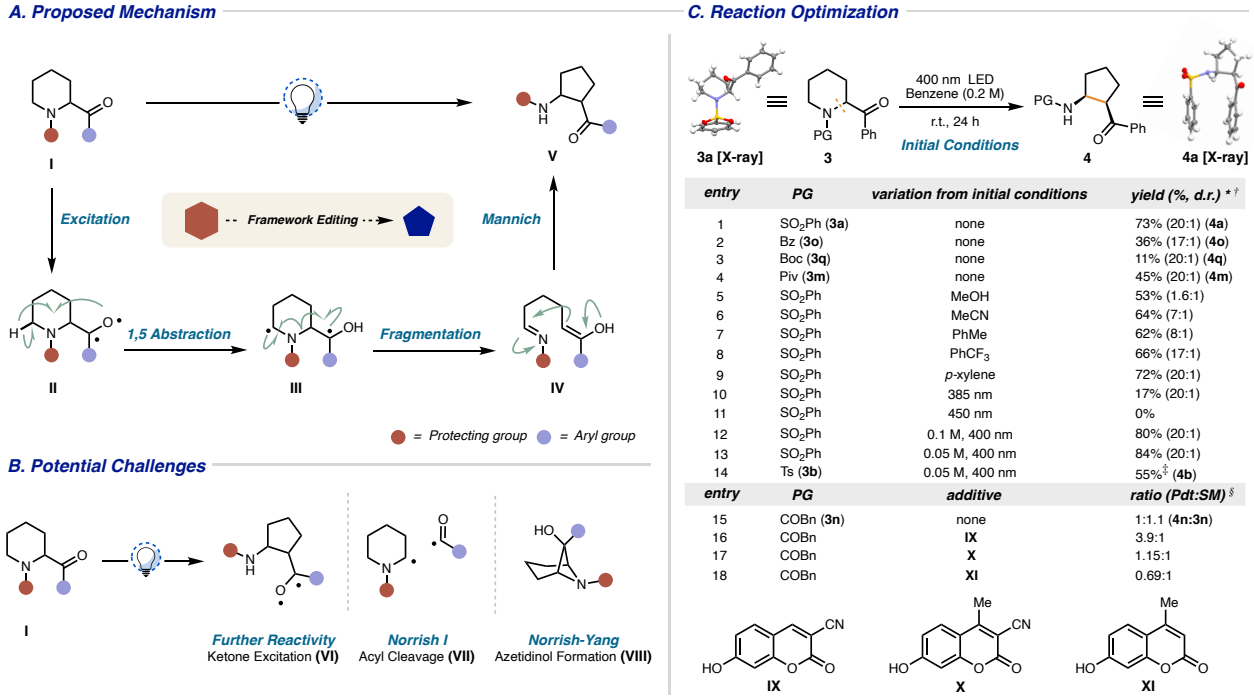

Figure 2. Reaction development. (A) Proposed mechanism for piperidine ring contraction. (B) Potential undesired side reactivity via Norrish Type I and Norrish–Yang cyclization processes. (C) Reaction optimization for light-mediated ring contraction. Reactions were carried out on a 0.05 mmol scale. Relative stereochemistry is depicted. *Yields were determined by ^{1}H NMR integration using Ph_3CH as an internal standard. †Diastereomeric ratio was determined by ^{1}H NMR integration of resonances corresponding to diastereomers in the crude mixture. ‡Reaction was carried out on a 1-gram scale in flow, with isolated yield of major diastereomer reported. §High throughput experimentation (HTE) conducted to identify 3-cyanoumbelliferone. Conversion was determined by LCMS analysis.

Despite the potential challenges associated with side- and over-reactions of our phenyl ketone substrate, on the basis of the anticipated differences in absorptivity for **I** and **V,** we reasoned that tuning the wavelength of light could selectively promote the desired reactivity while minimizing the photoreactivity of the resulting products. Gratifyingly, photo-irradiation of **3a** using a 400 nm blue LED lamp provided 1,2-disubstituted cyclopentane **4a** in 73% yield at room temperature (Fig. 2C, entry 1). Empirically, the photo-mediated ring contraction proceeded best with a 400 nm wavelength light source; longer wavelength

irradiation (centered at 450 nm; lower energy) did not result in any conversion, whereas shorter wavelength light sources (e.g., centered at 385 nm; higher energy), which more closely aligned with the calculated and measured absorptivity curves of *both* product and starting material, led to competing non-specific oligomerization. Sulfonyl groups on the piperidine nitrogen were uniquely effective in providing the desired product in good to high yields, presumably enhancing the intramolecular H-bond in **4a** that accounts for its stability under the reaction conditions. Other electron-withdrawing groups on the piperidine nitrogen, such as benzoyl, Boc, or pivaloyl (Fig. 2C, entries 2–4), resulted in lower yields of the ring contraction product. The choice of solvent was also critical. Benzene, which can enhance hydrogen bonding in **4a**, gave the highest yields and diastereoselectivity (*26*). Other solvents such as methanol (Fig. 2C, entry 5), acetonitrile (Fig. 2C, entry 6), toluene (Fig. 2C, entry 7), and trifluorotoluene (Fig. 2C, entry 8) led to diminished yields, and lower diastereoselectivity. Given the toxicity concerns of using benzene, we have also identified *p*-xylene as a serviceable solvent alternative (Fig. 2C, entry 9; see the *Supplementary Materials* for full solvent screen, and select substrates using *p*-xylene as the solvent). Lowering the concentration of the substrate also led to improvements in yield; a concentration of 0.05 M, which presumably slows the rate of competing unproductive intermolecular side reactions, was determined to be optimal. From these observations, we identified an optimized set of conditions for sulfonyl derivatives of the piperidine substrates, which afforded **4a** in 84% isolated yield and high diastereoselectivity (Fig. 2C, entry 13). The reaction could be carried out on gram-scale using flow chemistry (Fig. 2C, entry 14; see the *Supplementary Materials* for additional details). For substrates bearing other protecting groups, such as amide and carbamate substrates, we observed reduced conversion to the desired product. This observation was intriguing, as ostensibly the photoreactive phenyl ketone group in the starting substrates was conserved; we posited that changing the group on nitrogen (*e.g.*, sulfonyl to acyl or carbamoyl) could lead to discrete differences in the triplet state energy of the phenyl ketone We hypothesized that a photosensitizer or photocatalyst could improve the efficacy of the reaction, and thus we initiated a screen of 46 known photosensitizers and photocatalysts using amide substrate **3n**. 3-Cyanoumbelliferone (**IX**, Fig. 2C, entry 16) emerged as an effective additive that improved the efficiency of the reaction: piperidine **3m**, **3o**, **3s**, and **3t** were converted to their corresponding cyclopentylamines with improved yields (average of 11% increase, *vide infra*). The observed effect appears to be subtle and substrate dependent. Efforts to further understand the role of cyanoumberlliferone **IX** are ongoing.

Scope of the Photo-Mediated Ring Contraction

With optimized conditions in hand, the scope of the visible-light mediated ring contraction was explored (Fig. 3A). The generality of the group on the nitrogen atom was investigated first. Arylsulfonyl-derivatized piperidines featuring electron-withdrawing substituents, such as ketones (e.g., **3h**), esters (e.g., **3i**), and halogens (**3e**–**3g**) led to good to modest yields of the respective ring-contracted products. Likewise, arylsulfonyl-derivatized piperidines bearing electron-donating groups such as ethers (e.g., **3c** and **3d**) were also competent in the ring contraction transformation. The presence of a *p*-nitro substituent (**3j**) resulted in the complete recovery of starting material, likely resulting from photo-quenching (*27*–*29*). Although arylsulfonyl substituents on the piperidine nitrogen led to the highest ring contraction product yields, substrates bearing acyl (e.g., **3m**–**3p**), carbamoyl (**3q**), and urea-type groups (e.g., **3r**, **3s**) on the nitrogen also led to successful ring contraction in the presence of cyanoumbelliferone (**IX**) (Fig. 3A). Phosphoramidite-containing substrates (**3t**, **3u**) were also competent, providing the cyclopentane products

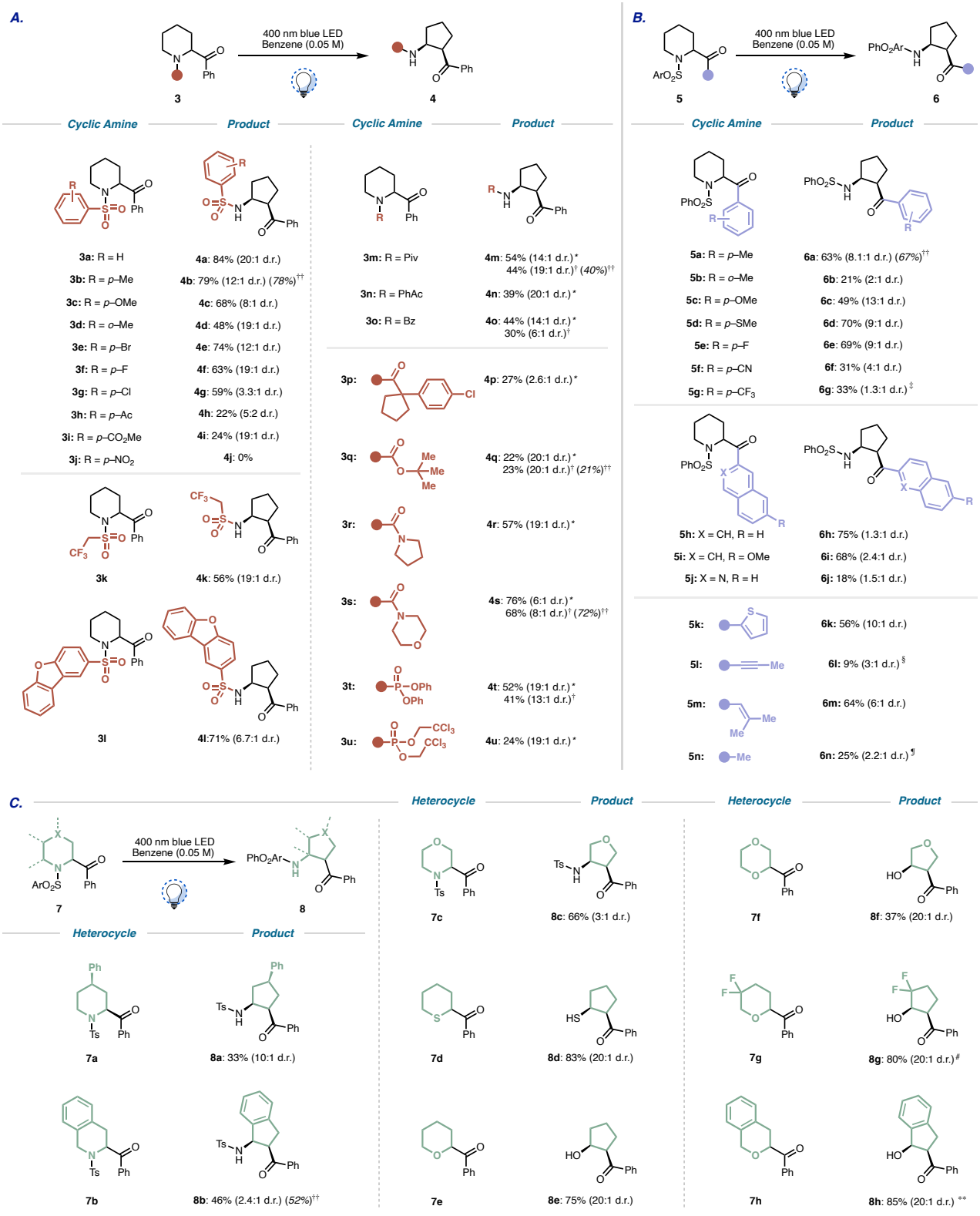

Figure 3. Scope of substrates in piperidine ring contraction. Reaction conditions: Starting material (0.2 mmol), benzene (0.05 M), 400 nm LED, 18–24 h. Isolated yields reported and relative stereochemistry shown. Diastereomeric ratio was determined by ^{1}H NMR integration of resonances corresponding to diastereomers in the crude. (A) Scope of protecting groups in ring contraction. *Additive **IX** (30 mol%) was added to the reaction mixture. †0.2 mmol scale

trials conducted in the absence of additive **IX**. (B) Scope of aryl ketone in ring contraction. [‡]Ring opened product following a subsequent Norrish Type II process is also observed. [§]Norrish–Yang azetidinol product observed in 12% (19% *brsm*). [¶]Reaction irradiated with a medium-pressure mercury lamp for 24 hours. (C) Scope of heterocyclic core in ring contraction. [#]Reaction conducted on a 0.14 mmol scale. [**]Reaction conducted on a 0.11 mmol scale. [††]Selected examples conducted on a 0.05 mmol scale using *p*-xylene (0.05 M) as a solvent. Yield was determined by ^{1}H NMR integration using Ph_3CH as an internal standard (see *Supplementary Materials* for more details).

in yields comparable to those observed for substrates bearing a sulfonyl group. In these cases, the phosphoramidyl group is easily removed under acidic conditions (*30*). The efficacy of the additive was also found to vary depending on the substrate, with the conversion of **3q** to **4q** being minimally affected upon adding **IX**. Here the persisting low yield likely involves reduced productive hydrogen atom transfer due to a preference for an unproductive conformation of the starting material (see *Supplementary Materials* for more details).

Next, we investigated the scope of the ring contraction with respect to the nature of the α-aroyl group (Fig. 3B). Here, the reaction was shown to be sensitive to sterics, with *p*-methyl substitution (**5a**) giving rise to higher yields and diastereoselectivity compared to the isomeric *o*-methyl substituted **5b**. Aryl ketones featuring electron-donating substituents, such as ethers (**5c**) and thioethers (**5d**), led to good yields and diastereoselectivity for the desired product. Halogen-containing α-aryl-ketone **5e** was also competent in the ring contraction chemistry, affording an additional functional handle for post-ring contraction modification. In comparison, electron-withdrawing groups such as *p*-CN and *p*-CF_3 (e.g., **5f**, **5g**) led to the formation of the desired product in modest yield and lower diastereoselectivity. This is likely the result of the increased acidity of the α-keto-proton in the product, which could undergo epimerization. On the basis of our calculations, epimerization through a retro-Mannich-Mannich pathway is unlikely *(vide infra*). Additionally, in the case of substrate **5g**, we observed an ensuing ring opening of the product through Norrish Type II cleavage, evidencing the potential over-reactivity of the cyclopentane products in some cases (see the *Supplementary Materials* for more details). Other aromatic ketones were also examined. For example, extended aromatic systems such as naphthalenyl ketones (**5h**) performed comparably, as did heteroaromatics such as thiophenyl ketones (see **5k**). While the conditions identified were optimized for α-aroyl groups, several substrates bearing non-aryl substituted ketones also participated successfully in the ring contraction transformation. Specifically, the desired products were observed for an alkynyl C(sp) bearing substrate (**5l**) and a vinyl C(sp^2) bearing substrate (**5m**). In the case of **5l**, the substantial decrease in yield can be attributed to a competing Norrish–Yang cyclization process leading to an azetidinol side product (see the *Supplementary Materials* for more details). Using more forcing, higher energy (mercury lamp) irradiation, alkyl C(sp^3) substituted ketone **5n** was converted to **6n** in 25% yield, highlighting, even in this case, the differential reactivity of the ketone groups in the starting material and product.

Substituted piperidines and several other saturated heterocycles were then examined for their propensity to undergo this type of ring contraction (Fig. 3C). Single substituents at the γ-position were tolerated (see **7a**) imparting stereocontrol. Notably, benzannulated substrates such as tetrahydroisoquinoline **7b** successfully underwent the ring contraction transformation, providing the corresponding amino indane scaffolds (i.e., **8b**) in good yields and under mild conditions. Additionally, upon irradiation of substrates containing a morpholine scaffold, the tetrahydrofuran heterocycle (**8c**) was formed. The ring contraction methodology was also extended beyond azacyclic frameworks to α-acylated thiane and tetrahydropyran (THP) derivatives. These were also competent substrates, leading to the

formation of cyclopentane thiol and alcohol products (see **8d–8h**), respectively. In the case of **7d**, formation of the resulting thiol (**8d**) could be viewed as the unveiling of a covalent modifier upon photo-irradiation.

Finally, we turned our attention toward the application of the ring contraction methodology to biologically active small molecules to demonstrate the potential for late-stage derivatization of drug candidates. Upon irradiation, MDMC (**9a**, stimulant), Rimiterol (**9b**, bronchodilator), Cathinone (**9c**, DAT reuptake inhibitor) (*31*) and Mefloquine (**9d**, antimalarial) derivatives underwent contraction to their corresponding cyclopentane isomers (Fig. 4A). In the case of **9d**, a ring-opened aldehyde side product was also observed, potentially arising from hydrolysis of the imine intermediate prior to Mannich-type ring closure. We speculate that these events are likely in this case because of the electron-deficient bis-trifluoromethylquinoline group in **9d**. The ring contraction transformation was also leveraged in peptide diversification (Fig. 4B). Here, glycine containing peptide **11** was converted to the corresponding amino cyclopentane (**12**), unveiling an H-bond donor. In this example, irradiation converts the α-peptide grouping to the corresponding β-amino ketone, accomplishing a non-intuitive peptide modification. Prospective applications include unveiling peptide-turn mimics upon irradiation.

Owing to the participation of cyclic ether derivatives in these light-mediated ring contractions, we have also explored this rearrangement in sugar editing (Fig. 4C). When subjected to 400 nm irradiation conditions, D-galactose-derived bis-acetonide **13** gave isomeric ring-opened product **14**. Here, the enol resulting from the Norrish Type II ring opening presumably tautomerizes to the aryl ketone and does not engage the lactone carbonyl group, offering a powerful targeted "digestion" of sugar derivatives.

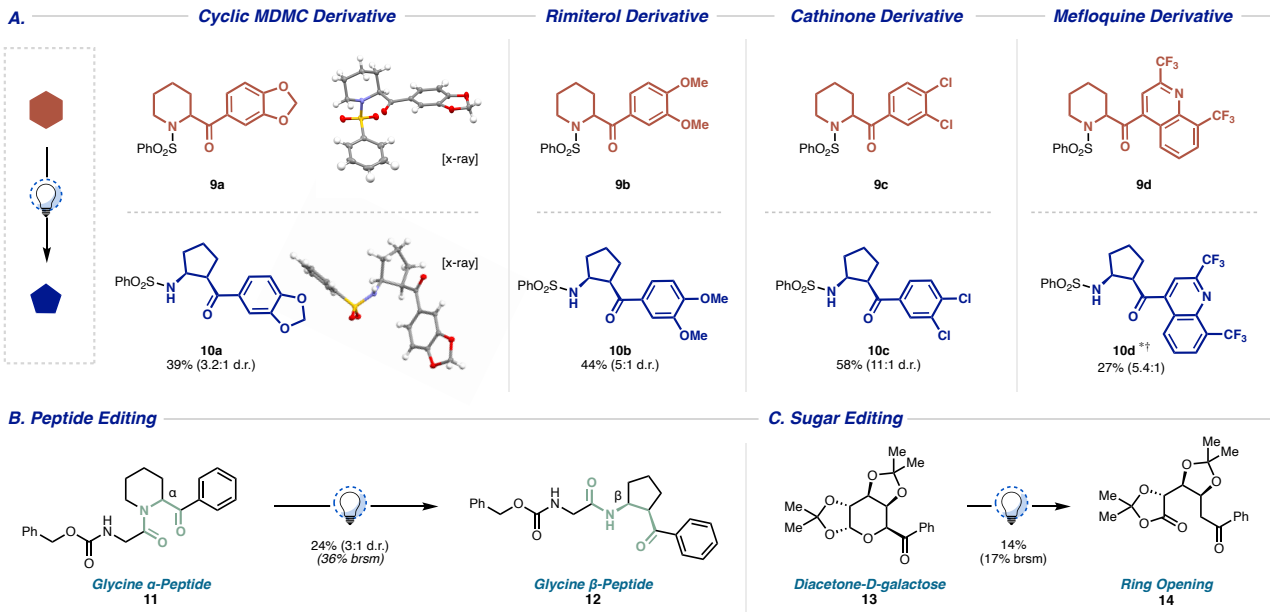

Figure 4. Applications toward biologically relevant compounds. (A) Selected examples of bioactive drug molecule contraction (B) Ring contraction mediated peptide editing (see *Supplementary Materials* for additional details). (C) Sugar editing enabled by targeted "digestion." Reaction conditions: Starting material (0.2 mmol), benzene (0.05 M), 400 nm LED, 24 h. Isolated yields reported and relative stereochemistry shown. Diastereomeric ratio was determined by ^{1}H NMR integration of resonances corresponding to diastereomers in the crude. *Reaction conducted on a 0.1 mmol scale where yield was determined by ^{1}H NMR integration using Ph_3CH as an internal standard, and d.r. was determined by ^{1}H NMR integration of resonances corresponding to diastereomers in the crude. †Ring opened product also observed in 4.5% yield (see *Supplementary Materials* for more details).

Computational Insight

To gain insight into the proposed mechanism and origin of stereoselectivity for these photo-mediated ring contractions, we have undertaken a computational study for the reaction of *N*-tosyl piperidine derivative **3b** (Fig. 6A). All of the quantum chemical calculations in the transition state modeling presented were performed using the *Gaussian 16* program (*32*). Geometry optimizations and frequency calculations were performed at the M06-2X/6-31+G** level of theory with the SMD model for implicit solvation by benzene (see the *Supplementary Materials* for more details) (*33–35*). We initially postulated that the positional selectivity for 1,5-HAT could be attributed to the greater hydricity and lower bond dissociation energy of the α-amino hydrogen atom (*see* ^{3}**3b** → ^{3}**A**, Fig. 5A). Using DFT calculations, we found that the more hydridic and polarity matched α-piperidinyl hydrogen atom had a HAT transition state 9.0 kcal/mol lower in energy than the potentially competing C–H abstraction at the γ-position (*36, 37*). The calculations also revealed a conformational preference in the transition state for the N–S bond wherein maximal separation is maintained between the carbonyl and sulfonyl oxygens (see the *Supplementary Materials* for additional details).

We also reasoned that the diastereoselective formation of the *cis*-disposed amino cyclopentane products (e.g., **4b**) would potentially result from a series of non-covalent interactions – such as π-stacking and hydrogen bonding – in the transition state for the Mannich-type ring closure. Computed transition state structures support the Mannich-type cyclization/C–C bond formation proceeding in concert with proton transfer from the enol moiety to the *N*-tosyl group, consistent with the proposal by Suarez and coworkers for the aldol-type cyclization in hexopyranose carbohydrates (*22*). Three scenarios could be envisaged that qualitatively support the experimentally observed diastereoselectivity (Fig. 5C, top right). In the first scenario, only the (*E*/*Z*) imine–enol is productive. This geometry arises when fragmentation of diradical intermediate ^{3}**A** occurs faster than acyl bond rotation (see ^{3}**A** orange bond). Alternatively, if interconversion of the (*Z*) and (*E*) forms for both the enol (C=C) and the imine (C=N) bonds is facile, then all four possible imine–enol double-bond geometries can be accessed in the Mannich cyclization. However, the requisite triplet 1,4-diradical conformer that would afford the (*Z*)-imine (Ts-axial) is high in energy and the contributions from a (*Z*)-imine geometry to the stereochemical outcome are expected to be negligible (see *Supplementary Materials* for complete discussion). We propose, therefore, that the most likely scenario is one in which the diradical is long-lived enough to allow acyl bond rotation and subsequent sampling of both enol diastereomers (*38, 39*). In this scenario, only the (*E*/*Z*) and (*E*/*E*) imine–enols are accessible and the energy differences between **TS-1**–**4** would determine the stereochemical outcome. The Boltzmann average of these four transition states predicted a ratio of 14:1 in favor of the *cis* cyclopentane isomer, in good agreement with the experimentally determined 12:1 ratio. The *cis* diastereoselectivity mainly originates from the energy difference between **TS-3** and **TS-4**, which could be rationalized by a shorter and presumably stronger hydrogen bond as well as a more staggered arrangement of substituents about the forming C–C bond in **TS-3** (^{1}**B** → ^{1}**4b**, Fig. 5C). Of note, the overall transformation of *N*-tosyl piperidine **3b** to either cyclopentane product was calculated to be exergonic (–4.2 kcal mol^{-1} for the **4b**, compared to –3.3 kcal mol^{-1} for the trans-isomer of **4b**).

Insight into the selective reactivity of the starting material compared to the product under the reaction conditions was also supported by DFT calculated and empirically measured absorption profiles of **3b** and **4b**. Even though the calculated λ_{max} values for the starting material and product (Fig. 5B, *top*) did

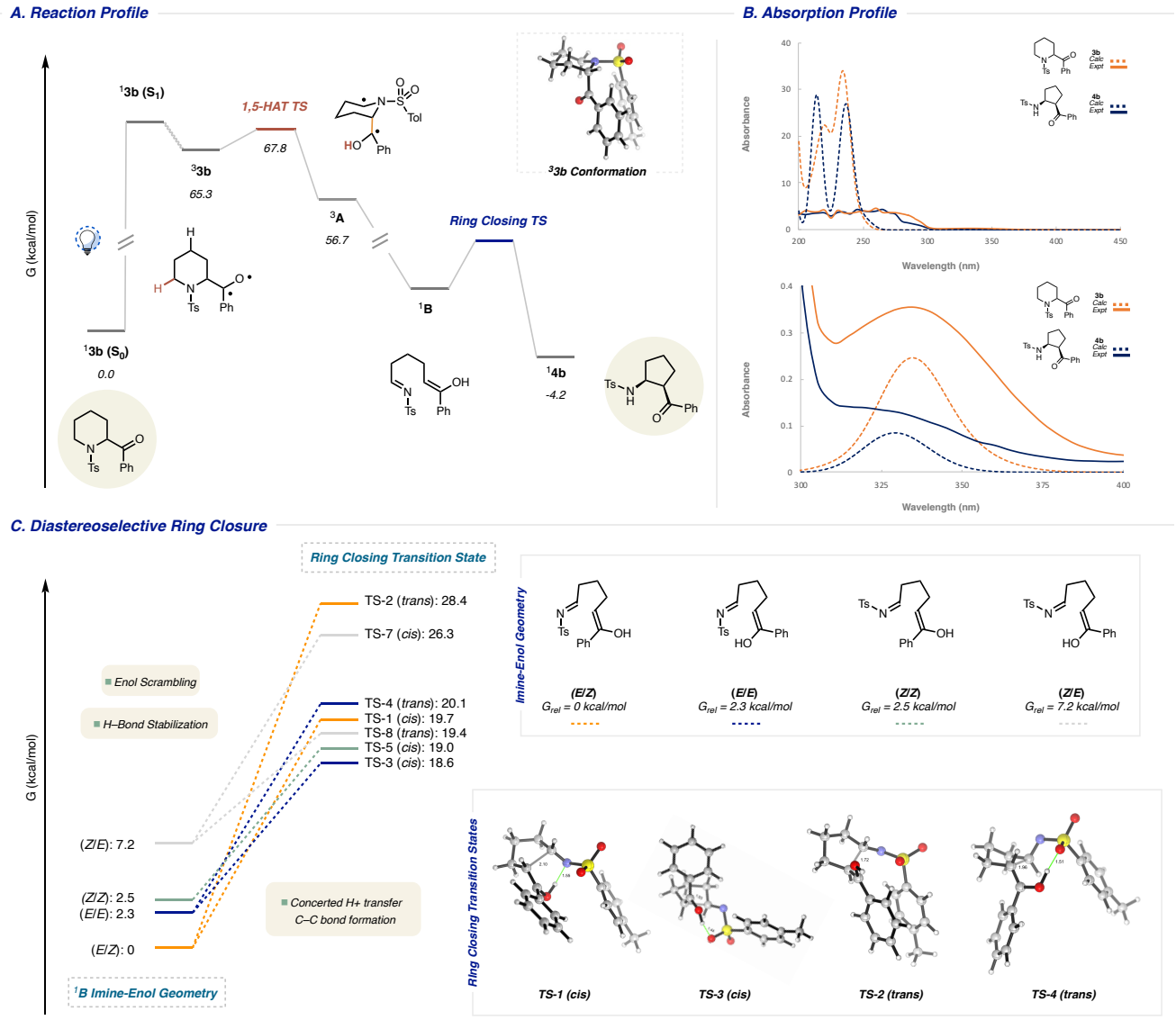

Figure 5. Computational studies on ring contraction mechanism. (A) Reaction profile for the piperidine ring contraction. (B) Experimentally and computationally (*normalized*) determined absorption profiles for the starting material (**3b**) and product (**4b**). (C) Imine-enol geometries and transition states calculated for the diastereoselective ring-closure.

not differ significantly, we observed secondary absorption peaks associated with the expected n→π* occurring from 300–375 nm (Fig. 5B, *bottom*). Here, a hypsochromic shift was observed for amino cyclopentane product **4b** relative to starting piperidine **3b**, likely accounting for the selective excitation of the starting material. Also observed empirically was an overall decrease in absorptivity for the product (e.g., ε_{340} = 48.0 L•cm^{-1}•mol^{-1} for **3b** vs. ε_{320} = 19.2 L•cm^{-1}•mol^{-1} for **4b**). While predictions and rationalizations of photochemical processes tend to focus on λ_{max} values, in our system, irradiation at λ_{max} would have led to indiscriminate reaction of both the starting materials and products. By focusing on the secondary, n→π*

absorption region of 300–375 nm, we are able to modulate the reactivity of the ketone group that is conserved in both the starting material and product by exploiting subtle differences in the absorbance wavelengths and extinction coefficients (see the *Supplementary Materials* for more details) (*40)*. Notably, the emission spectrum of the 400 nm light source slightly overlaps with the wavelength of light absorbed by the starting material but negligibly with the product. However, the empirically established optimal use of a commercially acquired 400 nm blue LED light source remains to be fully reconciled with the measured absorption values.

Toward a General Asymmetric Variant

Our insights into the observed diastereoselectivity for these transformations, which arises from highly organized transition states of an achiral imine-enol intermediate (as revealed from our calculations), combined with the successes of other powerful enantioselective photo-mediated processes (*41, 42*), inspired us to pursue enantioselective variants. We observed the formation of racemic product **4b** when enantioenriched **3b** was subjected to the ring contraction conditions, confirming that in this formal radical polar crossover process, the imine–enol intermediate is achiral. Therefore, we could circumvent the inherent challenges associated with stereocontrol of radical intermediates by effecting enantioselective closure of the achiral imine-enol intermediate under a two-electron reaction manifold (*43*). Given the ample literature precedent and predictive models for chiral phosphoric acid-catalyzed reactions of imines, we postulated that rate enhancement of the Mannich step would occur following imine protonation and attendant deprotonation of the enol, leading to an organized transition state favoring attack on one enantioface (see Fig. 6 and *Supplementary Materials* for more details). The combination of H-bonding and ion pairing that would be realized in this case was anticipated to yield enantioenriched Mannich products (Fig. 6) (*44–48*).

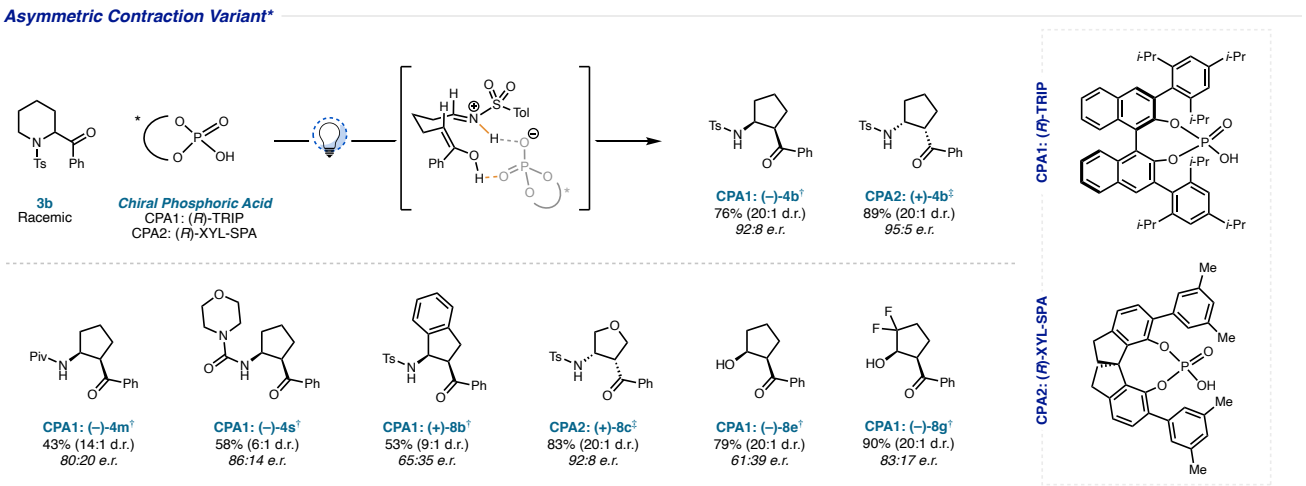

Figure 6. Development of an asymmetric ring contraction variant. *Reaction conducted on a 0.05 mmol scale where yields were determined by ^{1}H NMR integration using Ph_3CH as an internal standard, and d.r. was determined by ^{1}H NMR integration of resonances corresponding to diastereomers in the crude. For the major diastereomer, e.r. was determined by SFC analysis. †10 mol% (*R*)-TRIP (CPA1) used as chiral phosphoric acid. ‡10 mol% (*R*)-XYL-SPA (CPA2) used as chiral phosphoric acid.

Consistent with this hypothesis, ring contraction of **3b** with 10 mol% of (*R*)-TRIP (CPA1) as an additive provided (–)-**4b** in 92:8 e.r. (84% e.e.) with yields and diastereoselectivity consistent with those obtained under the standard reaction conditions for the formation of the racemate; using the SPINOL-derived phosphoric acid (*R*)-XYL-SPA (CPA2) gave (+)-**4b** in 95:5 e.r. (90% e.e.). Enantioselectivity, albeit modest, was also observed for amide, urea, THIQ, morpholine, and THP derivatives, giving rise to enantioenriched products **4m**, **4s**, **8b**, **8c**, **8e**, and **8g**, respectively.

Conclusion

Using a Norrish Type II reaction, we have established a versatile method for the scaffold remodeling of piperidines as well as other saturated heterocycles. The overall transformation is robust and the conditions tolerate a wide range of functional groups. Key to the success of these transformations is the "photo-protection" of a pendant ketone group in the product through intramolecular H-bonding, an observation supported by our experimental and computational findings. This reaction has been rendered enantioselective using chiral phosphoric acids.

References and Notes

(1) E. Vitaku, T. D. Smith, J. T. Njardarson, Analysis of the structural diversity, substitution patterns, and frequency of nitrogen heterocycles among U.S. FDA approved pharmaceuticals. *J. Med. Chem.* **57**, 10257–10247 (2014).

(2) A. S Lawrence, *Amines: Synthesis, Properties and Applications* (Cambridge University Press: New York, 2004).

(3) I. Coldham, D. Leonori, Synthesis of 2-arylpiperidines by palladium couplings of aryl bromides with organozinc species derived from deprotonation of N-boc-piperidine. *Org. Lett.* **10**, 3923–3925 (2008).

(4) K. R. Campos, A. Klapars, J. H. Waldman, P. G. Dormer, C.-Y. Chen, Enantioselective, palladium-catalyzed α-arylation of N-boc- pyrrolidine. *J. Am. Chem. Soc.* **128**, 3538–3539 (2006).

(5) S. Seel, T. Thaler, K. Takatsu, C. Zhang, H. Zipse, B. F. Straub, P. Mayer, P. Knochel, Highly diastereoselective arylations of substituted piperidines. *J. Am. Chem. Soc.* **133**, 4774–4777 (2011).

(6) W. Chen, L. Ma, A. Paul, D. Seidel, Direct α-C–H bond functionalization of unprotected cyclic amines. *Nat. Chem.* **10**, 165–169 (2018).

(7) S. J. Pastine, D. V. Gribkov, D. Sames, Sp_3 C–H bond arylation directed by amidine protecting group: α-arylation of pyrrolidines and piperidines. *J. Am. Chem. Soc.* **128**, 14220–14221(2006).

(8) P. Jain, P. Verma, G. Xia, J.-Q Yu, Enantioselective amine α-functionalizations via palladium-catalysed C–H arylation of thio-amides. *Nat. Chem.* **9**, 140–144 (2017).

(9) J. B. Roque, Y. Kuroda, J. Jurczyk, L.-P. Xu, J. S. Ham, L. T. Göttemann, C. A. Roberts, D. Adpressa, J. Saurí, L. A. Joyce, D. G. Musaev, C. S. Yeung, R. Sarpong, C–C cleavage approach to C–H functionalization of saturated aza-cycles. *ACS Catal*. **10**, 2929– 2941 (2020).

(10) A. Millet, P, Larini, E. Clot, O. Baudoin, Ligand-controlled β-selective C(sp_3)–H arylation of N-boc-piperidines. *Chem*. *Sci*. **4**, 2241–2247 (2013).

(11) R. Oeschger, B. Su, I. Yu, C. Ehinger, E. Romero, S. He, J. F. Hartwig, Diverse functionalization of strong alkyl C–H bonds by undirected borylation. *Science* **368**, 736–741 (2020).

(12) J. Topczewski, P. Cabrera, N. Saper, M. S. Sanford, Palladium-catalysed transannular C–H functionalization of alicyclic amines. *Nature* **531**, 220–224 (2016).

(13) K. R. Campos, P. J. Coleman, J. C. Alvarez, S. D. Dreher, R. M. Garbaccio, N. K. Terrett, R. D. Tillyer, M. D. Truppo, E. R. Parmee, The importance of synthetic chemistry in the pharmaceutical industry. *Science* **363**, 6424 (2019).

(14) K. A. Tehrani, K. V. Syngel, M. Boelens, J. Contreras, N. De Kimpe, D. W. Knight, Boron(III) bromide-induced ring contraction of 3-oxygenated piperidines to 2-(bromomethyl)pyrrolidines. *Tetrahedron Lett*. **41**, 2507–2510 (2000).

(15) A. Feraldi-Xypolia, D. G. Pardo, J. Cossy, Ring contraction of 3-hydroxy-3-(trifluoromethyl)piperidines: synthesis of 2-substituted 2-(trifluoromethyl)pyrrolidines. *Chem*. *Eur*. *J*. **21**, 12876 –12880 (2015).

(16) J. B Roque, Y. Kuroda, L. T. Göttemann, R. Sarpong, Deconstructive diversification of cyclic amines. *Nature* **564**, 244–248 (2018).

(17) F. Wang, Y. He, M. Tian, X. Zhang, X. Fan, Synthesis of α-formylated N-heterocycles and their 1,1-diacetates from inactivated cyclic amines involving an oxidative ring contraction. *Org*. *Lett*. **20**, 864–867 (2018).

(18) R. Ling, P. S. Mariano, A demonstration of the synthetic potential of pyridinium salt photochemistry by its application to a stereocontrolled synthesis of (+)-Mannostatin A. *J*. *Org*. *Chem*. **63**, 6072–6076 (1998).

(19) S. Wang, H. Wang, N. Tian, H. Yan, Insights for diastereoselectivity in synthesis of 2,3-dihydropyrroles by photochemical ring contraction of 1,4-dihydropyridines. *Tetrahedron Lett*. **65**, 152797 (2021).

(20) T. Gees, W. B. Schweizer, D. Seebach, An unusual rearrangement of a lithiated N-acyl-tetrahydroisoquinoline to an amino-indan skeleton and structural comparison of 3-amino-2-methylindan- and -tetrahydronaphthalene-2-carboxylic acids as possible building blocks for peptide-turn mimics. *Helv*. *Chim*. *Acta*. **76**, 2640–2653 (1993).

(21) D. Álvarez-Dorta, E. I. León, A. R. Kennedy, C. Riesco-Fagundo, E. Suárez, Sequential Norrish Type II photoelimination and intramolecular aldol cyclization of 1,2-diketones in carbohydrate systems: stereoselective sythesis of cyclopentitols. *Angew. Chem.* **120**, 9049– 9051 (2008).

(22) D. Álvarez-Dorta, E. I. León, A. R. Kennedy, A. Martin, I. Perez-Martin, C. Riesco-Fagundo, E. Suárez, Sequential Norrish Type II photoelimination and intramolecular aldol cyclization of α-diketones: synthesis of polyhydroxylated cyclopentitols by ring contraction of hexopyranose carbohydrate derivatives. *Chem. Eur. J.* **19**, 10312– 10333 (2013).

(23) K. A. Brameld, B. Kuhn, D. C. Reuter, M. Stahl, Small Molecule Conformational Preferences Derived from Crystal Structure Data. A Medicinal Chemistry Focused Analysis. *J. Chem. Inf. Model.* **48**, 1–24 (2008).

(24) E. V. Anslyn, D. A. Dougherty, "Photochemistry" in *Modern Physical Organic Chemistry* (University Science Books, 2006), pp. 935–1000.

(25) M. Oelgemöller, N. Hoffmann, Studies in organic and physical photochemistry – an interdisciplinary approach. *Org. Biomol. Chem.* **14**, 7392–744 (2016).

(26) C. Reichardt, T. Welton, "Solvent Effects on the Position of Homogeneous Chemical Equilibria" in *Solvents and Solvent Effects in Organic Chemistry* (Wiley-VCH, 2010), pp. 107–163.

(27) Q. Zheng, M. F. Juette, S. Jockusch, M. R. Wasserman, Z. Zhou, R. B. Altmana, S. C. Blanchard, Ultra-stable organic fluorophores for single-molecule research. *Chem. Soc. Rev.* **43**, 1044–1056 (2014).

(28) R. Dave, D. S. Terry, J. B. Munro, S. C. Blanchard, Mitigating unwanted photophysical processes for improved single-molecule fluorescence imaging. *Biophys J.* **96**, 2371–2381 (2009).

(29) J. H. M. van der Velde, J. J. Uusitalo, L. Ugen, E, M. Warszawik, A. Herrman, S. J. Marrink, T. Cordes, Intramolecular photostabilization via triplet-state quenching: design principles to make organic fluorophores "self-healing" *Faraday Discuss.* **184**, 221–235 (2015).

(30) P. G. M. Wuts, T. W. Greene, "Protection for the Amino Group" in *Greene's Protective Groups in Organic Synthesis* (Wiley, 2006), pp. 696–926.

(31) B. J. Yadav-Samudrala, J. M. Eltit, R. A. Glennon, Synthetic cathinone analogues structurally related to the central stimulant methylphenidate as dopamine reuptake inhibitors. *ACS Chem. Neurosci.* **10**, 4043–4050 (2019).

(32) M. J. Frisch, G. W. Trucks, H. B. Schlegel, G. E. Scuseria, M. A. Robb, J. R. Cheeseman, G. Scalmani, V. Barone, G. A. Petersson, H. Nakatsuji, H.; et al. Gaussian 16. Gaussian, Inc.: Wallingford, CT.

(33) Y. Zhao, D. G. Truhlar, The M06 suite of density functionals for main group thermochemistry, thermochemical kinetics, noncovalent interactions, excited states, and transition elements: two new functionals and systematic testing of four M06-class functionals and 12 other function. *Theor. Chem. Acc.* **120**, 215–241 (2008).

(34) A. V. Marenich, C. J. Cramer, D. G. Truhlar, Universal solvation model based on solute electron density and on a continuum model of the solvent defined by the bulk dielectric constant and atomic surface tensions. *J. Phys. Chem. B.* **113**, 6378–6396 (2009).

(35) R. F. Ribeiro, A. V. Marenich, C. J. Cramer, D. G. Truhlar, Use of solution-phase vibrational frequencies in continuum models for the free energy of solvation. *J. Phys. Chem. B.* **115**, 14556–14562 (2011).

(36) A. Padwa, An alkoxy radical as a model for the n, π* excited state. *Tetrahedron Lett.* **46**, 3465—3469 (1964).

(37) C. Walling, M. J. Gibian, Hydrogen abstraction reactions by the triplet states of ketones. *J. Am. Chem. Soc.* **87**, 3361—3364 (1965).

(38) M. Abe, Diradicals. *Chem. Rev.* **113**, 7011–7088 (2013).

(39) S. Muthukrishnan, J. Sankaranarayanan, T. C. S. Pace, A. Konosonoks, M. E. DeMichiei, M. J. Meese, C. Bohne, A. D. Gudmundsdottir, Effect of alkyl substituents on photorelease from butyrophenone derivatives. *J. Org. Chem.* **75**, 1393–1401 (2010).

(40) D. Staveness, J. L Collins III, R. C. MCAtee, C. R. J. Stephenson, Exploiting imine photochemistry for masked N-centered radical reactivity. *Angew. Chem. Int. Ed.* **58**, 19000–19006 (2019).

(41) R. Brimioulle, T. Bach, Enantioselective Lewis acid catalysis of intramolecular enone [2+2] photocycloaddition reactions. *Science*, **342**, 840–843 (2013).

(42) A. Holzl-Hobmeier, A. Bauer, A. Vieira Silva, S. M. Huber, C. Bannwarth, T. Bach, Catalytic deracemization of chiral allenes by sensitized excitation with visible light. *Nature*, **564**, 240–243 (2018).

(43) M. P. Sibi, S. Manyem, J. Zimmerman, Enantioselective radical processes. *Chem. Rev.* **103**, 3263–3295 (2003).

(44) J. M. M. Verkade, L. J. C. van Hemert, P. J. L. M. Quaedflieg, F. P. J. T. Rutjes, Organocatalysed asymmetric Mannich reactions. *Chem. Soc. Rev.* **37**, 29–41 (2008).

(45) J. Li, Y. Liu, S, Li, J. Ma, Chiral phosphoric acid-catalyzed direct asymmetric Mannich reaction of cyclic C-acylimines with simple ketones: facile access to C2 quaternary indolin-3-ones. *Chem. Commun.* **54**, 9151–9154 (2018).

(46) G. Yang, G. Li, J. Huang, D. Fu, X. Nie, X. Cui, J. Zhao, Z. Tang, Regioselective, diastereoselective, and enantioselective one-pot tandem reaction based on an in situ formed reductant: preparation of 2,3-disubstituted 1,5-benzodiazepine. *J. Org. Chem.* **86**, 5110–5119 (2021).

(47) J. P. Reid, L. Simon, J. M. Goodman, A practical guide for predicting the stereochemistry of bifunctional phosphoric acid catalyzed reactions of imines. *Acc. Chem. Res.* **49**, 1029–1041 (2016).

(48) J. P. Reid, M. S. Sigman, Holistic prediction of enantioselectivity in asymmetric catalysis. *Nature* **571**, 343–349 (2019).

(49) M. Akashi, N. Arai, T. Inoue, T. Ohkuma, Catalyst-controlled diastereoselection in the hydrogenation of heterocycloalkyl ketones. *Adv. Synth. Catal.* **353**, 1955–1960 (2011).

(50) A. R. Prosser, D. C. Liotta, One-pot transformation of esters to analytically pure ketones: methodology and application in process development. *Tetrahedron Lett.* **56**, 3005–3007 (2015).

(51) Z. Sun, N. Kumagai, M. Shibasaki, Photocatalytic α-acylation of ethers. *Org. Lett.* **19**, 3727–3730 (2017).

(52) A. Jakas, A. Visnjevac, I. Jeric, Multicomponent approach to homo- and hetero-multivalent glycomimetics bearing rare monosaccharies. *J. Org. Chem.* **85**, 3766–3787 (2020).

(53) G. Bashiardes, C. Cano, B. Mauze, Stereoselective cycloaddition of carbohydrates for the synthesis of new bicyclic oxazolidines bearing quaternary bridgehead. *Synlett.* **9**, 1425–1428 (2005).

(54) C. Ghobril, C. Sabot, C. Mioskowski, R. Baati, TBD-catalyzed direct 5- and 6-enolexo aldolization of ketoaldehydes. *Eur. J. Org. Chem.* **24**, 4104–4108 (2008).

(55) L. Fisera, I. Goljer, L. Jaroskova, Reaction of tetrahydrofuroisoxazoles with molybdenum hexacarbonyl. A new route to preparation of 3-substituted tetrahydro- and dihydrofuran derivatives. *Collect. Czech. Chem. Commun.* **53**, 1753–1760 (1988).

(56) T. Suwa, K. Nishino, M. Miyatake, I. Shibata, A. Baba, Synthesis of carbocycles by enone-selective reductions using organoiodotin hydride. *Tetrahedron Lett.* **41**, 3403–3406 (2000).

(57) Photoreactor supplier website: https://www.pennphd.com/product/10

(58) L. Simon, J. M. Goodman, A Model for the Enantioselectivity of Imine Reactions Catalyzed by BINOL-Phosphoric Acid Catalysts. *J. Org. Chem.* **76**, 1775–1788 (2011).

(59) C. Y. Legault. *CYLview, 1.0b (*Université de Sherbrooke, 2009).

(60) K. Roos, C. Wu, W. Damm, M. Reboul, J. M. Stevenson, C. Lu, M. K. Dahlgren, S. Mondal, W. Chen, L. Wang, R. Abel, R. A. Friesner, E. D. Harder, OPLS3e: Extending Force Field Coverage for Drug-Like Small Molecules. *J. Chem. Theory Comput.* **15**, 1863–1874 (2019).

(61) Schrödinger Release 2020-3, Schrödinger, LLC, New York, NY (2020).

(62) J. Tomasi, B. Mennucci, R. Cammi, Quantum Mechanical Continuum Solvation Models. *Chem. Rev.* **105**, 2999–3094 (2005).

(63) G. Scalmani, M. J. Frisch, Continuous surface charge polarizable continuum models of solvation. I. General formalism. *J. Chem. Phys.* **132**, 114110 (2010).

(64) J.-D. Chai, M. Head-Gordon, Long-range corrected hybrid density functionals with damped atom–atom dispersion corrections. *Phys. Chem. Chem. Phys.* **10**, 6615–6620 (2008).

(65) F. Weigend, R. Ahlrichs, Balanced basis sets of split valence, triple zeta valence and quadruple zeta valence quality for H to Rn: Design and assessment of accuracy. *Phys. Chem. Chem. Phys.* **7**, 3297–3305 (2005).

(66) A. D. Becke, Density-functional thermochemistry. III. The role of exact exchange. *J. Chem. Phys.* **98**, 5648–5652 (1993).

(67) C. Lee, W. Yang, R. G. Parr, Development of the Colle-Salvetti correlation-energy formula into a functional of the electron density. *Phys. Rev. B*. **37**, 785–789 (1988).

(68) S. H. Vosko, L. Wilk, M. Nusair, Accurate spin-dependent electron liquid correlation energies for local spin density calculations: a critical analysis. *Can. J. Phys.* **58**, 1200–1211 (1980).

(69) P. J. Stephens, F. J. Devlin, C. F. Chabalowski, M. J. Frisch, Ab Initio Calculation of Vibrational Absorption and Circular Dichroism Spectra Using Density Functional Force Fields. *J. Phys. Chem.* **98**, 11623–11627 (1994).

Acknowledgments: We acknowledge the help and support of the following people from Merck & Co., Inc., Kenilworth, NJ, USA (MSD): Shane W. Krska, Daniel DiRocco, Thomas W. Lyons, Dan Lehnherr, Louis-Charles Campeau, Alan Northrup, Nicholas K. Terrett, Emma R. Parmee, and Michael H. Kress for support of the Disruptive Chemistry Fellowship program; Umar Faruk Mansoor and Emily Corcoran for assistance with flow chemistry; Josep Sauri and Eugene Kwan for assistance in NMR structure elucidation; Dan Lehnherr, Mycah Uehling, Dipannita Kalyani, and Shishi Lin for assistance with high-throughput experimentation; Yuan Jiang, Taylor Johnson, Rosina Ayore, and Wilfredo Pinto for collecting HRMS data; Lisa M. Nogle, David A. Smith, Adam Beard, Miroslawa Darlak, and Mark Pietrafitta for reversed-phase purifications; Spencer McMinn and Lisa Nogle for chiral SFC purifications; and Nunzio Sciammetta, Andrew Musacchio, and Emily Corcoran for thorough review of the manuscript and helpful discussions. We also thank Audrey Reeves for collecting UV-Vis data, and Jose Roque and Jin Su Ham (Berkeley) for their helpful discussions. **Funding:** We thank the Disruptive Chemistry Fellowship program of Merck & Co., Inc., Kenilworth, NJ, USA (MSD) for gracious support of C.S.Y. and a part of the work disclosed in this manuscript. We thank the MRL Postdoctoral Research Program of Merck Sharp & Dohme Corp., a subsidiary of Merck & Co., Inc., Kenilworth, NJ, USA (MSD) for its generous support of M.C.L. and a part of the work disclosed in this manuscript. We thank the NIH for its funding for the 600 MHz cryoprobe (grant S10OD024998). R.S. is grateful to the NSF under the CCI Center for Selective C–H functionalization (CHE-1700982) and the National Institute of General Medical Sciences (R35GM130345A) for partial support of the work reported herein (Berkeley). **Author contributions:** J.J., M.C.L, C.S.Y. and R.S. conceived and designed the experiments reported in this work. J.J. M.C.L. and S.F.K. performed all the laboratory experiments. D.A. assisted in structural elucidation. Y.-h.L. designed and completed the density functional theory calculations. J.J., M.C.L., S.F.K., Y.-h.L., C.S.Y. and R.S. wrote the manuscript. C.S.Y. and R.S. directed the research. **Competing interests:** Richmond Sarpong is a paid consultant for Merck

Sharp & Dohme Corp., a subsidiary of Merck & Co., Inc., Kenilworth, NJ, USA. The authors declare no other competing interests. **Data and materials availability:** All reported data can be found in the manuscript or the Supplementary Materials. Requests for additional materials should be directed to the corresponding authors. X-Ray crystallographic data for **3a**, **4a**, **4m**, **9a**, **10a**, and (–)**4b** (CCDC 2061160, 2061161, 2061162, 2061169, 2061170, and 2071240 respectively) are available from the Cambridge Crystallographic Data Centre (https://www.ccdc.cam.ac.uk/).

Supplementary Materials

Materials and Methods

Supplementary Text

Figs. S1 to S30

Tables S1 to S7

References (*49*–*69*)